

Measurement of the internal flow in hydrogen bubbles using a model-based aberration correction

F. Bürkle*¹, A. Bashkatov², A. Babich², X. Yang², K. Eckert^{2,3}, J. Czarke¹, L. Büttner¹

¹ Technische Universität Dresden, Fakultät Elektrotechnik und Informationstechnik
Professur für Mess- und Sensorsystemtechnik, Helmholtzstraße 18, 01062 Dresden,
*E-Mail: florian.buerkle@tu-dresden.de

² Institute of Fluid Dynamics, Helmholtz-Zentrum Dresden-Rossendorf, Bautzner Landstraße 400,
01328 Dresden

³ Institute of Process Engineering and Environmental Technology, Technische Universität Dresden,
Helmholtzstr. 14, 01062 Dresden

Particle Image Velocimetry, Bildkorrektur, Elektrolyse, Wasserstoff
Particle Image Velocimetry, image correction, electrolysis, hydrogen

Summary

One challenge in electrolysis is the formation of hydrogen and oxygen bubbles on the electrodes, which leads to increased electrical resistance and efficiency losses. Efficient transportation of these bubbles away from the electrodes is crucial for optimizing electrolysis systems, which is affected by the flow inside and around the bubbles. The paper proposes a solution to overcome the challenges of studying the internal flow dynamics within the bubbles. The formation of the carpet of microbubbles between the electrode and growing gas bubble and their mutual coalescence under specific experimental conditions causes the injection of microdroplets. This allows for the visualization and tracking of the internal flow using Particle Image Velocimetry (PIV). The systematic measurement deviation induced by the curvature of the bubble was reduced by $\approx 50\%$ by the use of an analytical model. Measurements were performed during water electrolysis at different applied potentials, and the internal flow characteristics were analyzed. The results show that the applied potential has a significant impact on the internal flow structure. At low potentials, the main flow direction is vertical upwards, while higher potentials lead to a more complex flow pattern with a vortex at the bottom part of the bubble. These new insights will help to better understand the multifaceted dynamics of hydrogen bubbles during electrolysis for more efficient and sustainable hydrogen production.

Introduction

In recent years, the significance of hydrogen as a versatile process gas and a sustainable long-term energy storage solution has experienced a substantial surge. Traditionally, hydrogen production heavily relies on natural gas, but the need for a more environmentally friendly approach has led to the exploration of electrolysis using regenerative power sources. During this electrolysis process, hydrogen bubbles form on the electrodes, leading to an increase in Ohmic resistance between the electrodes, resulting in power and efficiency losses (Bashkatov et al. 2019, Angulo et al. 2020). Therefore, efficient transportation of these bubbles away from the electrodes is crucial. Understanding the growth and detachment dynamics of these bubbles is paramount for optimizing electrolysis systems.

Among the various factors influencing bubble growth and detachment, the role of convection both inside and outside the bubbles has gained attention. While the external flow driven by the thermocapillary and solutocapillary effect has been investigated employing Particle Tracking

Velocimetry (PTV) (Massing et al. 2019, Yang et al. 2018), the internal flow dynamics within the bubbles remain relatively unexplored. The lack of tracer particles, which are challenging to introduce into the bubbles, and the small size of the bubbles ($d < 1 \text{ mm}$), which induce significant spherical aberrations, have hindered detailed studies in this area.

This paper proposes a solution to overcome these challenges by utilizing a carpet of microbubbles that forms between the electrode and the growing hydrogen bubbles under specific experimental conditions. When these microbubbles coalesce with the hydrogen bubble, droplets are injected into the bubble, allowing for the visualization and tracking of the internal flow using PIV. The primary objective of this study is to present the flow characteristics inside the hydrogen bubbles during their growth under different applied potentials. The influence of the applied potential on the flow field inside the bubbles will be investigated and analyzed. An analytical model will be applied to the acquired data to demonstrate significantly reduced systematic deviations, thus improving the accuracy of the measurements.

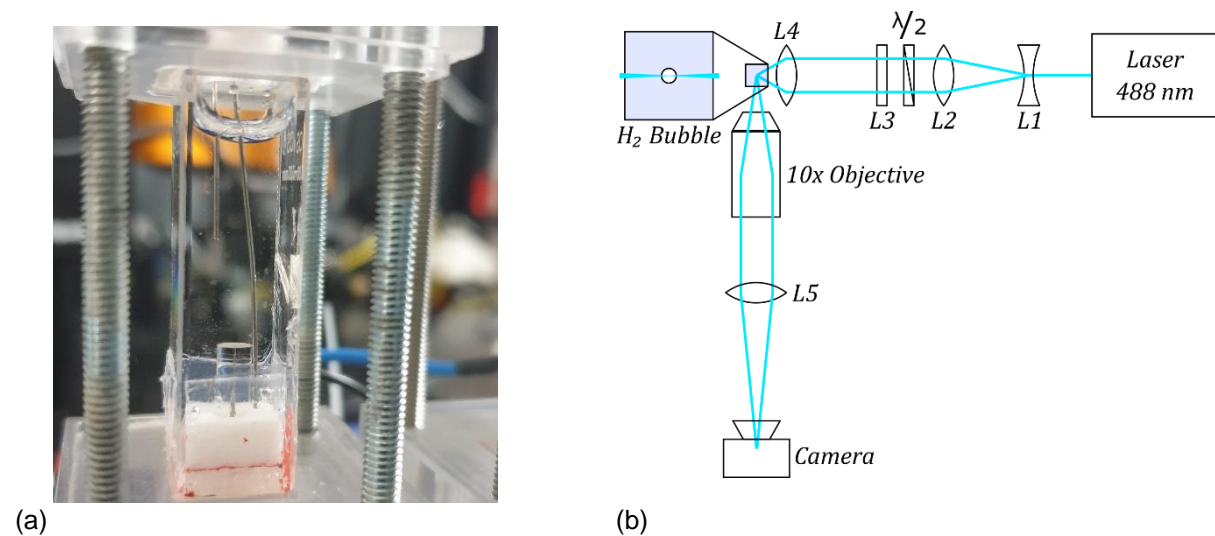


Fig. 1: (a) Image of the electrolysis cell. The hydrogen is produced in the center of the acrylic cylinder at the bottom where a platinum wire is inserted (b) Scheme of the micro-PIV measurement system.

Experimental Setup

The electrolysis cell is a cuvette with transparent sides (Fig. 1a). At the bottom of the cuvette a transparent cylinder with a platinum wire in the middle ($d = 100 \mu\text{m}$) is inserted which is used as the electrode (cathode) where hydrogen is produced. A cover on top of the cuvette prevents evaporation of the electrolyte. Two holes in the cover allow to insert an electrode (anode) where oxygen is produced, and a reference electrode for a stable potential during electrolysis. The electrolyte is an aqueous solution of sulfuric acid with a concentration of 0.1 mol/L .

The optical setup consists of a light sheet optic and an imaging optic (Fig. 1b). A laser ($\lambda = 488 \text{ nm}$, $P \leq 150 \text{ mW}$) was expanded by a Galilean telescope (L1 & L2). A $\lambda/2$ -waveplate rotates the linear polarization to have minimum reflection on the bubble surface. The light sheet was realized by a cylindrical lens (L3) and a convex lens (L4). In the center of the bubble the light sheet had a thickness of $d < 10 \mu\text{m}$. To visualize the flow a microscope consisting of a 10x magnification objective and a lens (L5, $f = 160 \text{ mm}$) images the hydrogen bubble on a camera. Depending on the maximum bubble size the resolution of the images was adapted. A constant frame rate of 1000 frames per second was chosen for the measurements.

Analytical Aberration Correction

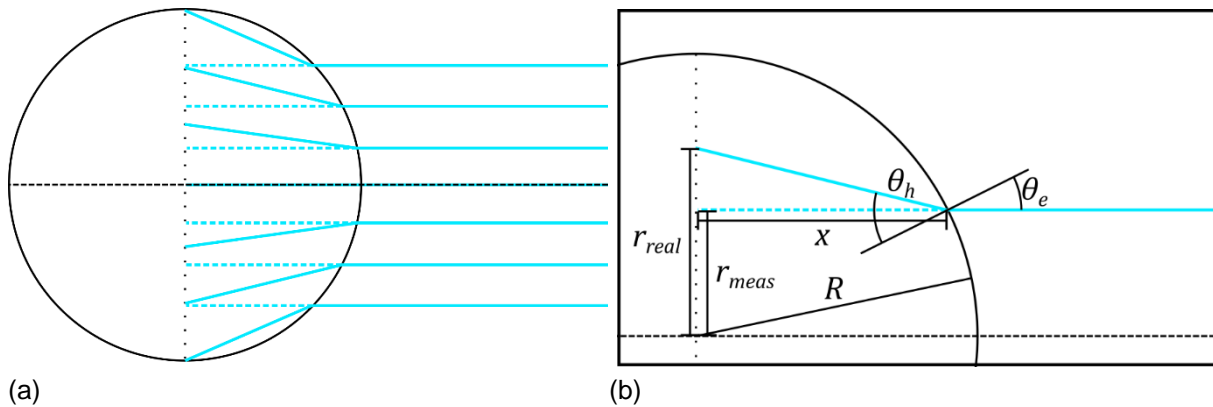


Fig. 2: (a) Scheme of the chief rays in an object-space telecentric setup. The microscope objective is on the right side. The position in the image plane is indicated with the dashed blue lines inside the bubble, the real position is indicated with the solid blue lines inside the bubble. (b) Close view at the transition of a ray from the bubble to the electrolyte.

Aberrations due to the curvature of the bubble lead to a significant systematic measurement deviation (Bilsing et al. 2022, Radner et al. 2020, Gao et al. 2021). As the bubbles are of sub-mm size a correction using an optical element is challenging. However, for object-space telecentric lenses, like the microscope objective used for the measurements, the aberrations can be corrected analytically, which has already been done for measurements in droplets (Minor et al. 2007). In this case the entrance pupil of the system is at infinity resulting in chief rays parallel to the optical axis in the object space. Furthermore, by the use of PIV light sheet, the plane where the light is coming from is known. When backpropagating the rays through the optical system, the intersection of the backpropagated ray and the light sheet with and without the bubble in the system can be calculated. A scheme of the chief rays passing the bubble surface at the bubble surface in a telecentric setup can be seen in Fig. 2a. The solid lines show

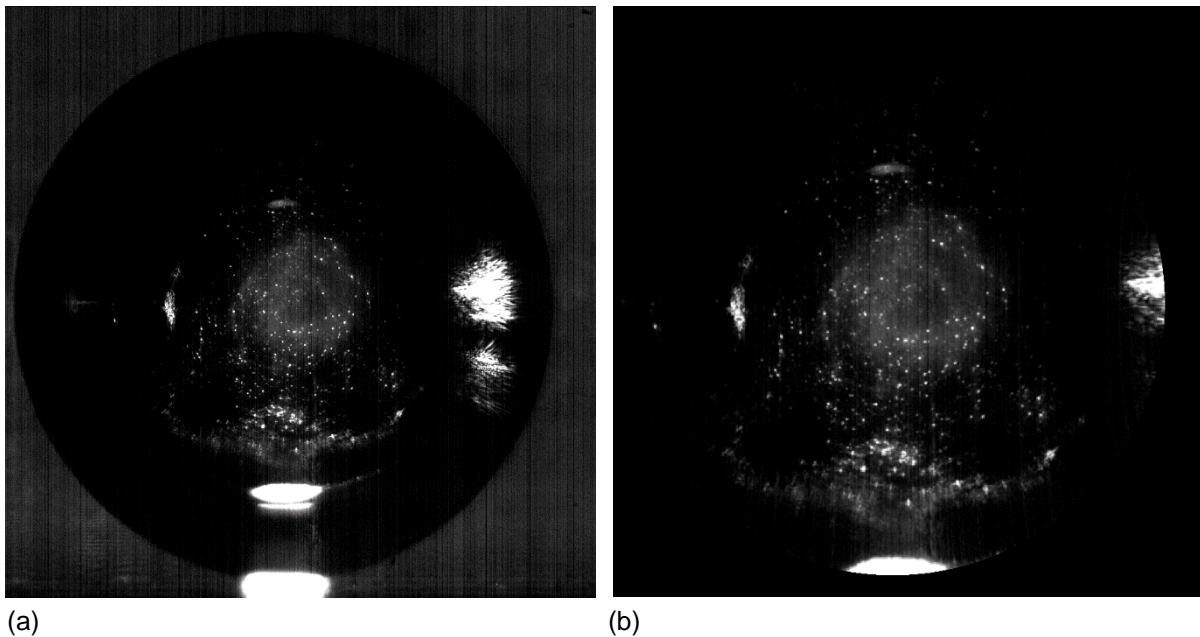


Fig. 3: Comparison of an image recorded by the measurement system (a) and the same image corrected with the analytical model (b). For data processing the pixels outside the bubble are blacked in the corrected image.

the real path of the light scattered at the droplets, whereas the dashed lines indicate the positions where it looks like the light comes from. In Fig. 2b the transition for one beam is shown with variables used for calculating the real position of the droplet. As the bubbles are rotationally symmetric, the position of the droplet is defined by the distance from the bubble center. The measured position is called r_{meas} , the real position is called r_{real} . With the further use of the refractive index of the electrolyte n and the bubble's radius R , the real position can be calculated to $r_{real} = r_{meas} + \Delta r$ with:

$$\Delta r = \tan \left[\sin^{-1} \left[n \cdot \sin \left[\tan^{-1} \left(\frac{r_{meas}}{\sqrt{R^2 - r_{meas}^2}} \right) \right] \right] - \tan^{-1} \left(\frac{r_{meas}}{\sqrt{R^2 - r_{meas}^2}} \right) \right] \cdot \sqrt{R^2 - r_{meas}^2}$$

The effect of the correction can be seen in Fig. 3: (a) represents a raw snapshot of an H₂ bubble and the electrolyte droplets inside, while (b) represents the same snapshot after performing the correction. It can be seen that there are no droplets in the outer region of the bubble. This is due to the spherical shape of the bubble which lets outside droplets appear closer to the bubble center. Especially at the bottom of the bubble this effect gets visible. The light scattered by the microbubble carpet reaches the camera sensor both directly through the electrolyte and through the bubble. The light traveling through the bubble seems to come from a position closer to the center. When the correction is applied, the light travelling through the bubble seems to come from the bubble surface, which implies that the analytical model is correct (Fig. 3b). Hence, the systematic deviation induced by the bubble can be corrected.

Measurement Results

Measurements were performed during water electrolysis at cathodic potentials between -3 V and -7 V. The internal flow for different potentials, averaged over 23 frames shortly before bubble detachment corrected with the analytical model can be seen in Fig. 4. The most significant difference is the greater bubble size right before the detachment when a higher potential is applied. Furthermore, it can be seen that the flow pattern in the central plane for -3 V and -5 V mostly looks similar with higher injection velocities at -5 V. A slight difference can be seen at the injection where some droplets are moving to the side. This effect gets stronger at -6 V and the formation of a vortex in the lower part of the bubble can be observed. This results in a flow countering the injection which leads to lower velocities at the injection compared to -5 V. For -7 V the vortex is more distinct and leads to even lower velocities at the injection. No valid vectors were calculated at the right and left part of the bubble.

Discussion

The applied potential has a significant impact on the internal flow geometry. For low potentials the main flow direction is vertical upwards due to the injection direction of the droplets. The fast deceleration of the flow after injection allows two different interpretations: Either there is no significant flow inside the bubble so the droplets are slowed down by the drag force. This leads to the assumption of rather small than big droplets. Another explanation is a downward flow slowing down the droplets, which can be seen clearly for higher potentials.

The flow pattern changes significantly with growing potential. The droplets are moving to the side which can only be explained by an existing flow inside the bubble. This flow is assumed to be driven by the electrolyte flow around the bubble. The thermocapillary or solutocapillary effects drive such a flow (Massing et al. 2019), known as Marangoni convection, which is stronger at higher potentials due to stronger temperature or species gradients in the vicinity of

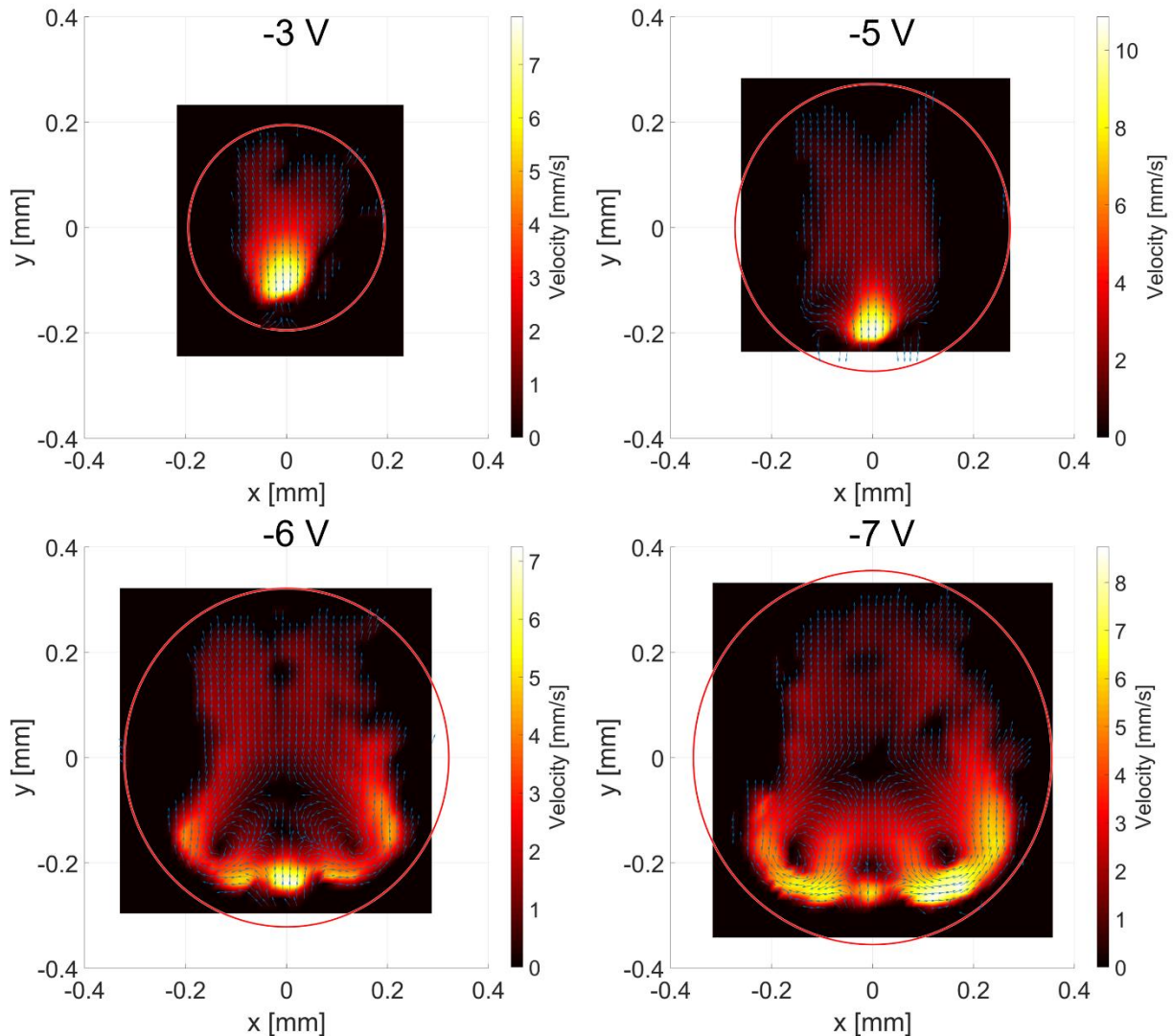


Fig. 4: Velocity fields in the central plane of the bubbles at different potentials. Invalid vectors were removed. The red circles indicate the shape of the bubbles.

the bubble bottom, ultimately caused by higher current densities. This explains the more distinct vortex at -7 V applied potential. The downward-facing flow reflects the presence of the strong Marangoni convection outside, which imposes a downward acting force keeping the bubble at the electrode longer, hence resulting in a less efficient process. Therefore, a lower potential might be desirable.

The lack of velocity vectors at the sides of the bubble can be explained by a lack of droplets in these regions. The droplets are injected vertically at the bottom and no flow transports them to the sides. Hence, a flow evaluation was not possible there.

In Fig. 5 the effect of aberration corrections can be seen: (a) shows the calculated velocity field without aberration correction and (b) with applied aberration correction. Significant systematic differences can be seen in the maximum velocity, which is about 50 % lower without aberration correction, and the velocity field is less symmetrical when calculated without aberration correction. Some flow structures are not evaluated correctly when using only the original image. This means that the analytical model allows for significant reduction of systematic measurement deviations which arise from the curvature of the bubble. Overall, the bubble-carpet coalescence, makes it possible to study the internal flows, when combined with the proposed optical system and analytical aberration correction. Future works would need to focus on the impact of these microdroplets on the dynamics of gas bubbles during water electrolysis.

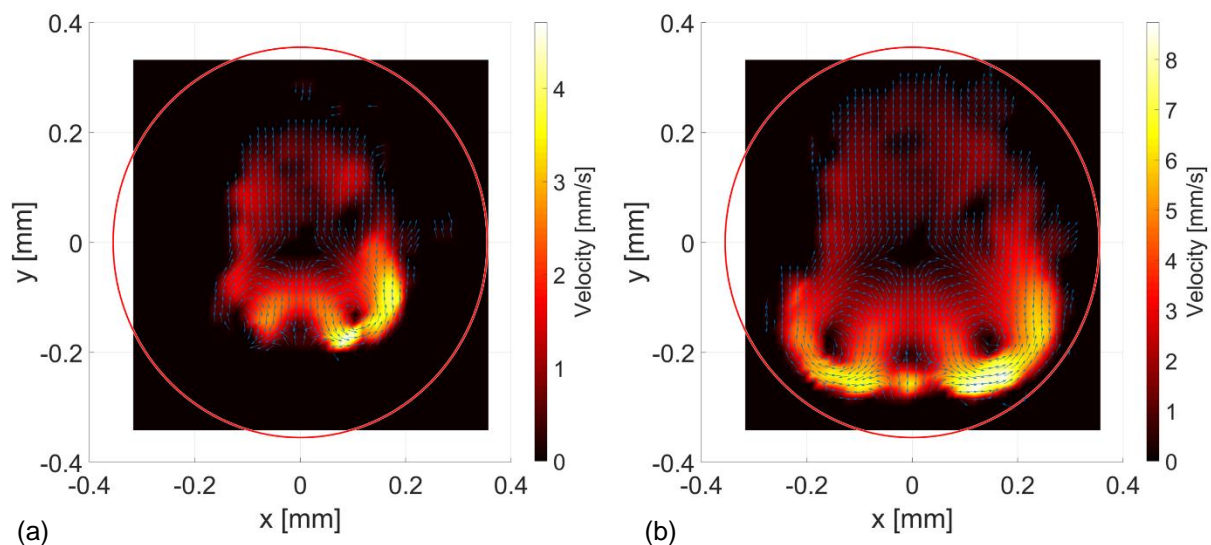


Fig. 5: Comparison of the velocity field calculated for a bubble at -7 V cathodic potential without correction (a) and with aberration correction (b).

Summary and Outlook

For the first time, worldwide unique measurements of the internal flow of a growing hydrogen bubble during electrolysis were performed. A model for aberration correction was developed and applied which reduced the systematic measurement deviation by 50 %. Furthermore, flow structures not visible without the correction can be evaluated when the correction is applied. A paradigm shift is expected by correcting the aberration induced by the curvature of the bubble by the use of adaptive optics, e. g. a deformable mirror (Radner et al. 2020, Bilsing et al. 2021, Bilsing et al. 2022). Three-dimensional measurements might be interesting in the case of a not rotationally symmetric setup, which usually is the case in industrial electrolyzers. One possibility to achieve those measurements is adding a spiral phase mask into the optical path (Teich et al. 2018). However, those experiments require more complex setups and volumetric illumination which would hinder the use of the analytical model.

Significant differences in the flow patterns were observed at different applied potentials. While the flow structure is quite simple for low potentials, a more complex structure with a vortex in the lower half is present for higher applied potentials. The droplets injected into the bubble can be used as a tool to investigate Marangoni convection inside the bubble. Future work will include simultaneous measurement of the internal and external flow and parameter studies. Experiments on macroelectrodes similar to this study will grant better understanding of industrial electrolysis.

By unraveling the internal flow dynamics of hydrogen bubbles generated during electrolysis, this research aims to provide valuable insights into optimizing the efficiency and performance of hydrogen production systems. The findings of this study will contribute to the broader efforts in advancing sustainable hydrogen technologies.

Acknowledgement

This work was partially funded by the German Research Foundation (DFG), project BU 2241/6-1, and the "Industrievereinigung für Lebensmitteltechnologie und Verpackung e. V. (IVLV)", the "Arbeitsgemeinschaft industrieller Forschungsvereinigungen "Otto von Guericke" e. V. (AiF)" and the Federal Ministry for Economic Affairs and Climate Action (IGF 22492 BR).

Literature

- A. Bashkatov, S. S. Hossain, X. Yang, G. Mutschke, K. Eckert, 2019:** "Oscillating Hydrogen Bubbles at Pt Microelectrodes", *Physical Review Letters* 123, 214503
- A. Angulo, P. van der Linde, H. Gardeniers, M. Modestino, D. F. Rivas, 2020:** "Influence of bubbles on the energy conversion efficiency of electrochemical reactors", *Joule* 4, 555-579
- J. Massing, G. Mutschke, D. Baczymalski, S. S. Hossain, X. Yang, K. Eckert, C. Cierpka, 2019:** "Thermocapillary convection during hydrogen evolution at microelectrodes", *Electrochimica Acta* 297, 929-940
- X. Yang, D. Baczymalski, C. Cierpka, G. Mutschke, K. Eckert, 2018:** "Marangoni convection at electrogenerated hydrogen bubbles", *Physical Chemistry Chemical Physics* 20, 11542
- H. Radner, J. Stange, L. Büttner, J. Czarske, 2020:** "Field programmable system-on-chip based control system for real-time distortion correction in optical imaging," *IEEE Transactions on Industrial Electronics*, 68 (4), 3370-3379
- C. Bilsing, H. Radner, S. Burgmann, J. Czarske, L. Büttner, 2022:** "3D Imaging with Double-Helix Point Spread Function and Dynamic Aberration Correction Using a Deformable Mirror", *Optics and Lasers in Engineering*, 154, 107044
- Z. Gao, H. Radner, L. Büttner, H. Ye, X. Li, J. Czarske, 2021:** "Distortion correction for particle image velocimetry using multiple-input deep convolutional neural network and Hartmann-Shack sensing", *Optics Express*, 29, 18669-18687
- G. Minor, P. Oshkai, N. Djilali, 2007:** "Optical distortion correction for liquid droplet visualization using the ray tracing method: further considerations", *Measurement Science and Technology*, 18, L23-L28
- C. Bilsing, H. Radner, L. Büttner, S. Burgmann, A. Metzmacher, J. Czarske, 2021:** "Particle Tracking Velocimetry mit dynamischer Aberrationskorrektur für 3D-Strömungsmessungen in Tropfen mit dynamischer Oberfläche", 28. Fachtagung „Experimentelle Strömungsmechanik“, Bremen, 7
- M. Teich, L. Büttner, J. Czarske, 2018:** „Adaptives Helix Partikel Tracking in verdunstungsinduzierten Wassertropfenströmungen“, 26. Fachtagung „Experimentelle Strömungsmechanik“, Rostock, 20